Bioconjugate Chemistry

Article

pubs.acs.org/bc

Production of Site-Specific Antibody–Drug Conjugates Using Optimized Non-Natural Amino Acids in a Cell-Free Expression System

Erik S. Zimmerman, Tyler H. Heibeck, Avinash Gill, Xiaofan Li, Christopher J. Murray, Mary Rose Madlansacay, Cuong Tran, Nathan T. Uter, Gang Yin, Patrick J. Rivers, Alice Y. Yam, Willie D. Wang, Alexander R. Steiner, Sunil U. Bajad, Kalyani Penta, Wenjin Yang, Trevor J. Hallam, Christopher D. Thanos, and Aaron K. Sato*

Sutro Biopharma, Inc. 310 Utah Ave Suite 150 South San Francisco, California 94080, United States

Supporting Information

ABSTRACT: Antibody–drug conjugates (ADCs) are a targeted chemotherapeutic currently at the cutting edge of oncology medicine. These hybrid molecules consist of a tumor antigen-specific antibody coupled to a chemotherapeutic small molecule. Through targeted delivery of potent cytotoxins, ADCs exhibit improved therapeutic index and enhanced efficacy relative to traditional chemotherapies and monoclonal antibody therapies. The currently FDA-approved ADCs, Kadcyla (Immunogen/Roche) and Adcetris (Seattle Genetics), are produced by conjugation to surface-exposed lysines, or partial disulfide reduction and conjugation to free cysteines, respectively. These stochastic modes of conjugation lead to heterogeneous drug products with varied numbers of drugs conjugated across several possible sites. As a consequence, the field has limited understanding of the relationships between the site and extent of drug loading and ADC attributes such as efficacy, safety, pharmacokinetics, and immunogenicity. A robust platform for rapid production of ADCs with defined and uniform sites of drug conjugation would enable such studies. We have established a cell-free protein expression system for production of antibody drug conjugates through site-specific incorporation of the optimized non-natural amino acid, para-azidomethyl-L-phenylalanine (pAMF). By using our cell-free protein synthesis platform to directly screen a library of aaRS variants, we have discovered a novel variant of the *Methanococcus jannaschii* tyrosyl tRNA synthetase (TyrRS), with a high activity and specificity toward pAMF. We demonstrate that site-specific incorporation of pAMF facilitates near complete conjugation of a DBCO-PEG-monomethyl auristatin (DBCO-PEG-MMAF) drug to the tumor-specific, Her2-binding IgG Trastuzumab using strain-promoted azide–alkyne cycloaddition (SPAAC) copper-free click chemistry. The resultant ADCs proved highly potent in *in vitro* cell cytotoxicity assays.

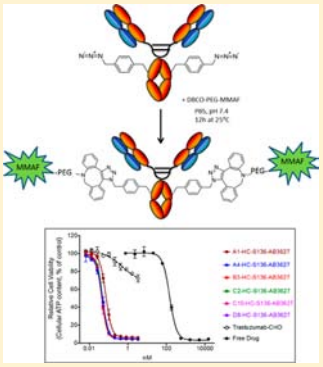

INTRODUCTION

The recent FDA approvals and positive clinical performances of antibody–drug conjugates (ADCs) such as Adcetris (Seattle Genetics) and Kadcyla (Immunogen/Roche) have exemplified the promise of this targeted oncology therapy.[1,2] There are technical challenges, however, associated with drug conjugation to proteins using naturally occurring amino acids, primarily due to heterogeneous degrees and location of drug loading as well as conjugate stability.[3] In order to reduce product heterogeneity and improve ADC therapeutic properties, several groups have reported site-directed approaches that utilize substituted cysteines, enzymatic modification of engineered glutamine residues using transglutaminase, or modification of carboxy-terminal aldehyde tagged proteins for conjugation.[4−6] Thiol-based coupling exhibits limited stability of the thiomaleimide linker–drug conjugate due to maleimide exchange with albumin, free cysteine, or reduced glutathione in the plasma.[3] Nevertheless, with properly selected conjugation sites, site-specific ADCs can exhibit potency and stability on par with randomly conjugated ADCs while exhibiting superior therapeutic index and pharmacokinetics.[4−7] An alternative to the aforementioned site-specific ADC technologies is to use site-specific incorporation of non-natural amino acids with chemical side chains that are compatible with bio-orthogonal conjugation chemistry. Non-natural amino acid (nnAA) based approaches offer a site-specific solution to making ADCs that eliminates the heterogeneity and instability inherent in conjugates generated stochastically through endogenous lysine or cysteine residues.[8] ADCs produced using a nnAA-based bio-orthogonal chemistry approach are not subject to the limitations of maleimide exchange and disulfide shuffling observed for cysteine substituted ADCs, nor do they require the additional enzymatic processing steps required for transglutaminase or aldehyde tag strategies.

The essential componentry of most nnAA incorporation systems consists of an aminoacyl tRNA synthetase (aaRS) that

Received: October 28, 2013
Revised: January 15, 2014
Published: January 17, 2014

charges a specific tRNA with a nnAA. The aaRS-tRNA pair must be orthogonal with respect to the host cell or expression system in which they are employed. That is, the nnAA-specific synthetase must not recognize any host tRNAs or cognate amino acids, and the orthogonal tRNA must not be aminoacylated by any host aaRS. Additionally, the orthogonal tRNA anticodon is often mutated to recognize a stop or nonsense codon.[9] Repurposing of nonproteinogenic codons, such as the amber stop codon TAG, enables incorporation of a nnAA at any site in a protein through substitution of the mRNA coding sequence to TAG.[10,11] Many different aaRS-nnAA pairs from several heterologous hosts have been evolved using methods pioneered by Schultz and colleagues.[9,12−16] This approach involves redirecting the specificity of the *Methanococcus jannaschii* tyrosyl tRNA synthetase toward a nnAA and TAG-decoding tRNA through directed evolution and genetic selection in *E. coli*.[9,17−19] This groundbreaking work essentially expanded the genetic code of *E. coli* by recoding the amber stop codon TAG to encode for a nnAA. Since these landmark studies, over 80 nnAAs have been encoded into proteins in several industry-standard prokaryotic and mammalian in vivo protein expression systems.[15,20−30] In particular, nnAAs with bio-orthogonal reactive chemical side chains can be used as a chemical "handle" to conjugate a payload to discrete sites in a protein.[8,21,31] This approach allows one to add functionality to proteins through direct conjugation of fluorescent or radioactive labels, photoactivatable markers, pharmacokinetic modifying PEGs, or chemotherapeutic agents.

We and others have employed site-specific nnAA incorporation to conjugate chemotherapeutic cytotoxins to tumor antigen-binding IgGs.[8] These antibody−drug conjugates (ADCs) are highly efficacious in cell killing assays as well as *in vivo* tumor xenograft models.[8] It has been demonstrated that both the degree and site of drug loading determine ADC efficacy and pharmacokinetics.[4,5,7] It also stands to reason that the exact site of conjugation and number of drugs conjugated will influence other ADC properties such as the stability, conjugation efficiency, immunogenicity, antigen binding, and internalization. The ability to optimize these parameters should yield site-specific ADCs with several advantages over ADCs produced by stochastic conjugation methods.

Open cell free synthesis (OCFS) is a rapid, cost-effective, virus-free process for manufacturing of therapeutic proteins based on scalable in vitro transcription/translation[32,33] In 2009, Goerke and Swartz successfully employed an *M. jannaschii* aaRS-tRNA system in a similar cell free protein synthesis system to incorporate the nnAA para-azido-L-phenylalanine (pAzF) into dihydrofolate reductase for conjugation to a fluorescent dye. However, the low overall product yield, nnAA incorporation efficiency, and conjugation efficiency together indicated a need for significant improvements in order for nnAA incorporation in OCFS to be a viable production system.[34] Otting and co-workers have recently reported successful incorporation of a variety of nnAAs proteins, using an *M. jannaschii* TyrRS-derived synthetase/nnAA pairs in an *E. coli*-based cell-free expression system.[35,36] This system proved to be quite efficient for incorporation of the nnAAs para-acetyl-L-phenylalanine, bipyridyl-phenylalanine, and L-(7-hydroxycoumarin-4-yl) ethylglycine, but rather inefficient for incorporation of the click-chemistry compatible nnAA, pAzF.[35] We thus set out to develop a robust platform for cell-free based expression of nnAA-containing proteins with superior properties for strain-promoted azide−alkyne cycloaddition-based (SPAAC) copper-free click bio-orthogonal conjugation.

In an effort to increase conjugation efficiency and the resultant site-specific drug-loading, we have designed and synthesized the optimized azide-containing nnAA; para-azidomethyl-L-phenylalanine (pAMF), which we hypothesized would enable more rapid conjugation kinetics compared to pAzF. We successfully utilized our OCFS system as a high-throughput screening platform to redirect specificity of the *M. jannaschii* TyrRS toward pAMF. This aaRS-tRNA-nnAA combination and copper-free click conjugation chemistry [37] has enabled the production of homogeneous ADCs with drug-to-antibody ratio (DAR) values approaching the theoretical limit of two drugs per antibody. This platform will enable rapid and exhaustive analysis of the relationships between conjugation site, drug loading, and efficacy for any candidate ADC scaffold. Lead ADC candidates can be rapidly produced in high quantity due to the highly scalable nature of our expression platform.[32] ADCs produced with this methodology could yield more active and diverse drug products, as well as offer a significant advantage for regulatory analysis and manufacturing due to superior product homogeneity.

EXPERIMENTAL PROCEDURES

Small Molecule Conjugation Kinetics. First-order kinetics at 25 °C, ionic strength 0.5 M (KCl), and 0.005% Tween-20 in phosphate buffer (20 mM sodium phosphate, pH 7.4) were determined under pseudo-first-order conditions in triplicate, using a SpectraMax M5 plate reader with 96-well polystyrene plates (Molecular Devices; Sunnyvale, CA). The decrease in absorbance of the strained cyclooctoalkyne at 306 nm was monitored in the presence of increasing concentrations of pAzF or pAMF. The second-order rate constants were calculated according to k_{cat} (M^{-1} s^{-1}) = k_{obs}/[Azido].

Library Construction. Synthetic DNA oligonucleotides were used to amplify overlapping PCR fragments of the *Methanococcus jannaschii* TyrRS. PCR primers encoded for the desired mutations at library residues Tyr32 (Ala, Leu, Val, or Thr), Leu65 (Ala, Ile, Leu, or Val), Phe108 (Phe, Trp, or Tyr), Gln109 (Gln, Ile, Leu, or Met), Asp158 (Ala or Gly), and Ile159 (Ala, Gly, Ser, or Val). PCR primers for each positional library variant were mixed at equimolar ratios before addition to the PCR amplification reaction at a final concentration of 1 μM. Individual PCR fragments were isolated by agarose gel electrophoresis and purified using a gel extraction kit (Zymo Research; Irvine, CA). The individual fragments were assembled by standard overlapping PCR procedures to yield a full-length PCR product encoding a library of synthetase variants. This PCR product library was digested with restriction enzyme BsaI and ligated into a T7 promoter-driven expression vector pYD317. The ligation reaction was transformed into *E. cloni* 10G competent cells (Lucigen; Middleton, WI) and the plasmid DNA from 2 mL cultures of 96 individual transformed colonies was purified with a DNA miniprep kit (Qiagen; Valencia, CA) and sequenced using a T7 promoter-specific primer to confirm the designed diversity of the library. Upon confirmation of library quality and coverage, 1760 colonies were used to inoculate 2 mL cultures for plasmid miniprep. 1760 DNA minipreps were performed to provide the plasmid DNA template to drive tRNA synthetase expression in OCFS reactions.

CF-Based aaRS Screening. Cell free expression reactions were performed as previously described,[33,38] with the following

modifications: the base extract *E. coli* strain SBJY001 was transformed with a plasmid driving constitutive expression of an optimized amber suppressor tRNA derived from *M. jannaschii*. This transformed strain was grown in high density fermentation and prepared as an extract as described previously to make extract SBEZ023. Using extract SBJY001, lacking amber suppressor tRNA, 1760 OCFS reactions were performed, at the 100 μL scale in 96 well microtiter plates incubated for 12 h at 30 °C to produce the individual aaRS variant proteins. Four microliters of the synthetase production OCFS reaction was added to a 20 μL GFP K49TAG reporter OCFS reaction, using a blend of extract SBJY001 and SBEZ023 (85%:15% respectively), in 384 well black microtiter plates in either the presence or absence of 1 mM pAMF. After 12 h of expression at 30 °C, the end point GFP fluorescence signal of the entire reaction (excitation at 476 nm, emission at 510 nm) was measured on a SpectraMax M5 fluorescence plate reader (Molecular Devices; Sunnyvale, CA).

Cell Free Protein Expression. The antibodies were expressed in a cell-free protein synthesis reaction as described in refs 32,33 with the modifications described below. A cell-free extract blend (85% SBJY001: 15% SBEZ023) was treated with 50 μM iodoacetamide for 30 min at RT (20 °C) and added to a premix containing all other components except for IgG heavy and light chain DNA. The final concentration in the protein synthesis reaction was 30% cell extract, 1 mM pAMF, 5uM pAMFRS, 2 mM GSSG, 2 mM amino acids (except 0.5 mM for Tyrosine and Phenylalanine), 2 μg/mL Trastuzumab light chain DNA, 8 μg/mL Trastuzumab-(His)6 heavy chain DNA containing an amber codon at the S136 position. Cell free reactions were initiated by addition of plasmid DNA of heavy and light chain and incubated at 30 °C for 12 h on a shaker at 650 rpm in 48-well Flower plates (m2p laboratories; Hauppauge, NY). The reaction was incubated further at 4 °C for 6 h until it was processed for purification.

High Throughput IMAC Purification. Following cell free protein synthesis, the mixture was transferred to a 96-well plate (Dynablock, 2 mL) and centrifuged at 5000×*g* for 15 min at 4 °C. Purification of IgG from the cell-free supernatant was carried out by using IMAC Phytips (Phynexus) containing 40 μL resin. This resin bed was pre-equilibrated in IMAC equilibration buffer (50 mM Tris pH 8.0, 300 mM NaCl, 10 mM Imidazole) and the clarified supernatant was pipetted up and down 10 times through equilibrated IMAC Phytips at a flow rate of 4.2 μL/min. The bound protein was washed with IMAC equilibration buffer, and then eluted with 125 μL IMAC elution buffer (50 mM Tris pH 8.0, 300 mM NaCl, 500 mM Imidazole).

Purification of IgG for MS Analysis. 30 mL of crude cell-free material was clarified using centrifugation after 2:1 dilution with 100 mM sodium phosphate, 150 mM sodium chloride, pH 7.4. The resultant supernatant was then applied to a 1 mL HiTrap MabSelect SuRE (GE Healthcare Life Sciences; Piscataway, NJ) column for IgG capture according to the manufacturer's recommendation. The IgG was eluted with 0.1 M citric acid, 300 mM L-arginine-HCl, pH 3.0, and the resulting pool adjusted to pH 4.6 with 1 M Tris, pH 9.0. Subsequently, this pool was processed on a 1 mL HiTrap Capto adhere (GE Healthcare Life Sciences; Piscataway, NJ) column that had previously been equilibrated with 0.1 M Tris-citrate, 300 mM L-arginine-HCl, pH 4.6. The IgG contained in the flow-through was collected and then buffer exchanged via dialysis into PBS.

DBCO-PEG-MMAF Conjugation. The Trastuzumab variants were conjugated to an exemplary cytotoxic agent, MMAF, using a constrained cyclooctyne reagent. In brief, DBCO-PEG-MMAF (ACME Bioscience; Palo Alto, CA) was dissolved in DMSO to a final concentration of 5 mM. The compound was diluted with PBS to 1 mM and then added to the purified protein sample in IMAC elution buffer to final drug concentration of 100 μM and a final pAMF-incorporated IgG concentration of 10 μM (10:1 molar ratio of drug-linker:IgG). This mixture was incubated at RT (25 °C) for 16 h. Reaction was stopped by adding sodium azide to final concentration of 1 mm and buffer exchanged using zeba plates (Thermo Scientific) equilibrated in 1× PBS. Filtrate was then passed through a MUSTANG Q plate (Pall Corp.) to remove endotoxin.

Protein Quantitation. LabChip GXII (Caliper Life-Sciences/Perkin-Elmer) was used for analysis of purified IgG and aaRS concentration and purity, using the Protein Express Chip assay. Assay reagents were prepared per manufacturer guidelines and run using Low Sensitivity mode. Samples (2 μL) were mixed with 7 μL Protein Express Sample Buffer using a 96-well PCR plate, denatured at 65 °C for 10′ and mixed with 32 μL Milli-Q water. For quantification, a Trastuzumab or *M. jannaschii* TyrRS standard curve ranging from 500 to 10 μg/mL was prepared in an identical manner to the analyzed samples. The 96-well PCR plate was run on the LabChip GXII and samples were quantified using LabChip GX software v 3.1 (Caliper LifeSciences/Perkin-Elmer).

Fidelity Analysis of Trastuzumab-CF S136pAMF by LC-MS/MS. The protein was diluted in 4 M guanidine hydrochloride and buffered with 100 mM ammonium hydroxide (pH 8.3). The disulfide bonds were reduced in the presence of 6 mM dithiothreitol at 37 °C for 45 min following alkylation with iodoacetamide (12 mM, at room temperature for 30 min). After dilution with 100 mM ammonium hydroxide to a final guanidine hydrochloride concentration of 1 M, trypsin was added at a 1:30 protease:substrate ratio and incubated for 15 h (overnight) at 37 °C. After digestion, trifluoroacetic acid was added to 0.5% (v/v). The digest mixture was then concentrated and desalted using a Macro peptide trip cartridge (Bruker-Michorm Inc., Auburn, CA) and eluted with 80% acetonitrile/water (0.1% trifluoroacetic acid) in fractions of one bed volume (50 μL). Fractions containing peptide (as determined by A_{280}) were combined and lyophilized. Peptides were reconstituted in 0.1% trifluoroacetic acid.

All mass spectra were acquired on an Agilent Technologies 6520 Accurate-Mass Q-TOF LC/MS system equipped with an HPLC-Chip system using a large capacity peptide chip (Agilent Technologies, Zorbax 300SB C18, 5 μm; separation column: 150 mm × 75 μm, enrichment column: 9 mm, 160 nL). Digest peptides were injected onto the enrichment column at 5% mobile phase B (acetonitrile, 0.1% formic acid; mobile phase A: 0.1% formic acid in water) and washed on column with the flow diverted to waste for 5 min and a flow rate of 2 μL/min. After washing, the enrichment column was switched in line with the separation column and the gradient increased to 15% mobile phase B over 4 min, and then increasing over 33 min to 80% (nano pump flow rate: 0.25 μL/min). The column was washed for 3 min at 90% mobile phase B before re-equilibrating for 5 min at 5%. Spectra were acquired first with an MS only method followed by a data dependent MS/MS method with a preferential list containing the theoretical *m*/*z* values for target peptides (containing pAMF, Phe, Tyr, and Gln in the sequence

dx.doi.org/10.1021/bc400490z | *Bioconjugate Chem.* 2014, 25, 351−361

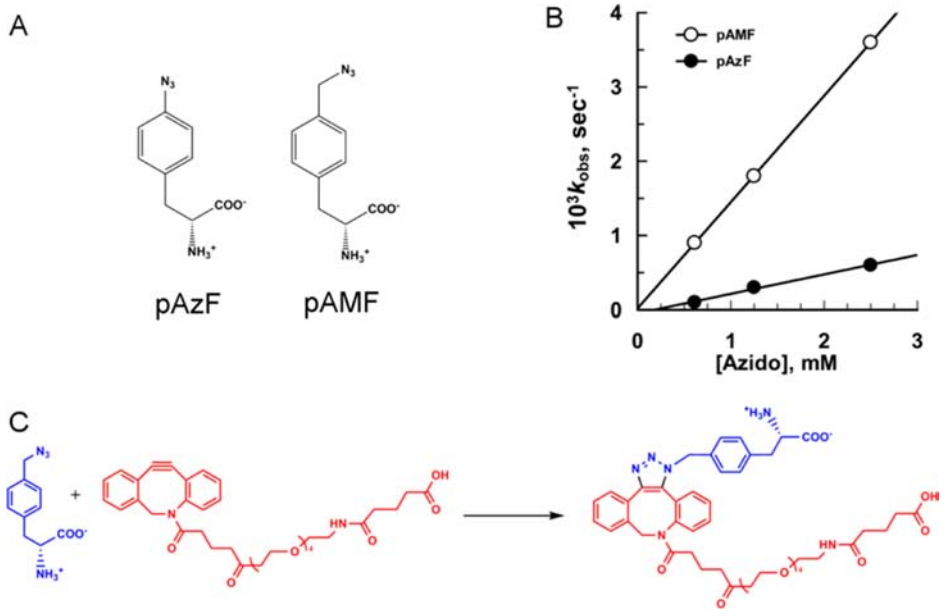

Figure 1. Strain-promoted azide−alkyne cycloaddition (SPAAC) reaction kinetics. (A) The non-natural amino acids para-azido-L-phenylalanine (pAzF) or para-azidomethyl-L-phenylalanine (pAMF) were incubated at increasing concentrations with a 10-fold molar excess of dibenzocyclooctyl-polyethylene glycol (DBCO-PEG) compound in a SPAAC reaction. (B) The formation of conjugated product was measured by decrease in absorbance of the strained DBCO-PEG at 306 nm. The second-order rate constants were calculated according to k_{cat} (M^{-1} s^{-1}) = k_{obs}/[Azido]. (C) SPAAC reaction between an azido-containing non-natural amino acid and DBCO-PEG measured in (B).

in place of pAMF or Phe). Blank injections of 50% acetonitrile:water were run between each digest acquisition. The Fragmentor was set at 180 V for all runs.

Data analysis was completed with manual and automated methods. The Molecular Feature Extraction function in MassHunter Qualitative was used to search for any inclusion of pAMF, Tyr, or Gln in a tryptic digest of Trastuzumab-CF S136F at any Phe in the sequence. Potential misincorporation events were treated as variable modifications in the search settings. All cysteines were assumed to be alkylated (fixed modification) and no other modifications were searched. The profile data of the MS-only acquisition was search down to a minimum peak interesting of 100 counts (about 2−3 times the average noise level of the instrument). Following automatic data extraction all peptides containing potential misincorporation events were manually checked. To determine maximum amount of measurable misincorporation, the monoisotopic peak height of all observed charge states for each Phe-containing tryptic peptide were manually determined at the apex of the peptide elution (as determined by an extracted ion chromatogram) and divided into the amount of noise adjacent to the isotopic cluster. Where a misincorporation event was observed, the monoisotopic peak intensity of this ion would be used in place of the noise measurement. The fidelity percentage was determined by the following formula: (1 − noise/monoisotopic ion intensity) × 100. The final value was taken as the average of all observed charge states for a given peptide.

Determination of Drug to Antibody Ratio. Spectra were acquired on an Agilent Technologies 6520 Accurate-Mass Q-TOF LC/MS system equipped with a 1200 series Binary SL pump and dual spray source. Water with 0.1% formic acid and a 20:80 isopropanol:acetonitrile solution with 0.1% formic acid were used as mobile phase A and B, respectively. Samples were separated over an PLRP-S polymeric reversed-phase column (50 × 2.1 mm, 5 μm, 4000 Å from Aglient Technologies) with loading at 0.2 mL/min in 10% mobile phase B followed by a 5 min on-column wash with the flow diverted to waste. Afterward at jump to 30%B over 1 min a 2.5%B/min gradient was run to 45%B, followed by a 5%B/min gradient to 60%B. The column was then cleaned at 95%B followed by three, 30 s sawtooth gradients between 95% and 10%B. Spectra were acquired at the slowest flow rate in high resolution mode with the Fragmentor set to 370 V.

Data were analyzed using MassHunter Qualitative. Mass spectra were combined over the entire elution range of all conjugates after determination of each conjugate's elution profile as determined by an extracted ion chromatogram of its most abundant ions. This step is critical since different drug-conjugates do not always coelute, but also do not resolve chromatographically (especially when using reversed-phase chromatography). Combining spectra over just a portion of the entire elution range for all conjugates will bias the drug to antibody ratio (DAR) determination. Mass spectra were deconvoluted using the Maximum Entropy deconvolution algorithm. The DAR for all samples was determined as a weighted average of the decovoluted mass spectrum peak intensities for each conjugate.

In Vitro Cytotoxicity Assay. The cell killing activity of ADCs was measured by a cell-based proliferation assay. SKBR3 were obtained from ATCC and maintained in DMEM: /Nutrient F-12 Ham (50:50), high glucose (Cellgro-Mediatech; Manassas, VA) supplemented with 10% heat-inactivated fetal bovine serum (Hyclone; Thermo Scientific; Waltham, MA), 2 mM glutamax (Invitrogen; Carlsbad, CA), and 1× penicillin/streptomycin (Cellgro-Mediatech; Manassas, VA). Adherent cells were washed twice with calcium and magnesium-free Phosphate Balanced Saline (PBS), harvested with HYQTASE (Hyclone; Thermo Scientific; Waltham, MA). A total of 1 × 10^3 cells in a volume of 40 μL were seeded in each well of a 96-well half area flat-bottom white Polystyrene plate. The cells were allowed to adhere overnight at 37 °C in a CO_2 incubator. ADC variants were formulated at 2×

dx.doi.org/10.1021/bc400490z | Bioconjugate Chem. 2014, 25, 351−361

concentration in DMEM/F12 medium and filtered through sterile SpinX cellulose acetate filtered 2 mL centritube (Corning Costar, Cat#8160). 40 μL of filter sterilized ADCs were added into treatment wells and plates were cultured at 37 °C in a CO_2 incubator for 120 h. For cell viability measurement, 80 μL of Cell Titer-Glo reagent (Promega Corp. Madison, WI) was added into each well, and plates were processed according to product instructions. Relative luminescence was measured on an ENVISION plate reader (Perkin-Elmer; Waltham, MA). Relative luminescence readings were converted to % viability using untreated cells as controls. Data was fitted with nonlinear regression analysis, using log-(inhibitor) vs response-variable slope, four-parameter fit equation using GraphPad Prism software.

RESULTS

Structural Optimization of a nnAA. In order to develop an efficient and robust ADC production platform, we sought to explore azide-containing nnAAs with novel chemical structures that could enhance the rate of SPAAC reactions.[37,39] Since the *M. jannaschii* system had been used previously to incorporate para-substituted phenylalanine derivatives, we used pAzF as our starting point. We reasoned that addition of a methylene group between the phenyl ring and the para-position azide group would position the azido group further away from the potentially electron-withdrawing phenyl ring, thus favoring the SPAAC reaction. In order to test this hypothesis, we synthesized both pAzF and pAMF (Figure 1A). These compounds were reacted at increasing concentrations with a 10-fold molar excess of dibenzocyclooctyl-polyethylene glycol (DBCO-PEG) compound (Figure 1C), and the formation of conjugated product measured by decrease in absorbance of the strained DBCO at 306 nm. The strained DBCO group has been shown to enable efficient, orthogonal reaction with azide groups in biological systems.[40] The second-order rate constants were calculated according to k_{cat} (M^{-1} s^{-1}) = k_{obs}/[Azido]. In support of our hypothesis, the reaction rate for pAMF was 7-fold higher than that for pAzF (Figure 1B). This finding validated the pursuit of a pAMF-specific aaRS to enable cotranslational incorporation of this enhanced nnAA. Recently, Brewer and colleagues reported in vivo incorporation of pAMF, which was found to be a sensitive and stable vibrational probe of local protein environments and, importantly, less prone to reduction of the azide group than pAzF.[41]

Discovery of a pAMF-Specific aaRS. We used rational design, based on the crystal structure of the wild-type *M. jannaschii* TyrRS (PDB ID 1J1U), to construct a TyrRS active site library of limited diversity that could be sampled, in its entirety, in a single 2000 clone screen, as this would allow for rapid proof of concept in a matter of days. The library design strategy was to create space in the amino acid binding pocket of *M. jannaschii* TyrRS (Figure 2A) to accommodate the bulkier nnAA pAMF. Moreover, we altered residues at that would eliminate selectivity for the hydroxyl group of the cognate substrate, tyrosine, and excluded highly charged or bulky amino acids from several positions based on the steric clashes predicted to occur with pAMF modeled into the TyrRS active site. A total of six residues in the active site were randomized to the amino acids indicated in Figure 2A and B. The theoretical diversity of the designed library was 1536 possible unique variants. Overlap extension PCR was performed with equimolar concentrations of primers specific for each designed mutation to construct a defined library of aaRS variants. This PCR

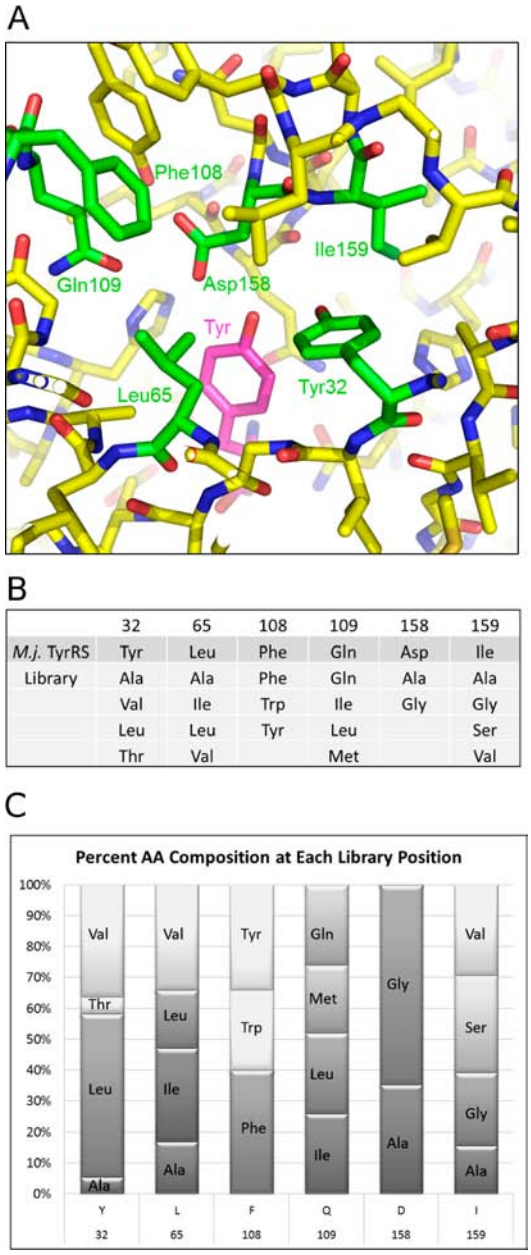

	32	65	108	109	158	159
M.j. TyrRS	Tyr	Leu	Phe	Gln	Asp	Ile
Library	Ala	Ala	Phe	Gln	Ala	Ala
	Val	Ile	Trp	Ile	Gly	Gly
	Leu	Leu	Tyr	Leu		Ser
	Thr	Val		Met		Val

Figure 2. TyrRS library design and analysis. (A) The amino acid binding pocket of *M. jannaschii* TyrRS with tyrosine (PDB ID# 1J1U). Residues in green were mutated to the amino acids indicated (panel B) using overlap extension PCR to construct a library of TyrRS variants to be screened for redirected specificity toward the nnAA pAMF. (C) The sequences of 96 library clones were analyzed to determine the relative amino acid frequency at the designated library positions.

product was ligated into a T7-promoter driven expression vector, pYD317, and used to transform *E. coli*.[32] The final aaRS coding sequence contained an in-frame, carboxy terminal hexahistidine tag to facilitate downstream protein purification. Plasmid DNA from 96 individual clones was sequenced to assess library coverage and diversity. The relative ratios of amino acids at the library positions were essentially as designed with the exception of a bias toward valine and leucine at position 32, which was originally designed to be composed of an equal distribution of valine, leucine, alanine, and threonine (Figure 2C).

dx.doi.org/10.1021/bc400490z | *Bioconjugate Chem.* 2014, 25, 351−361

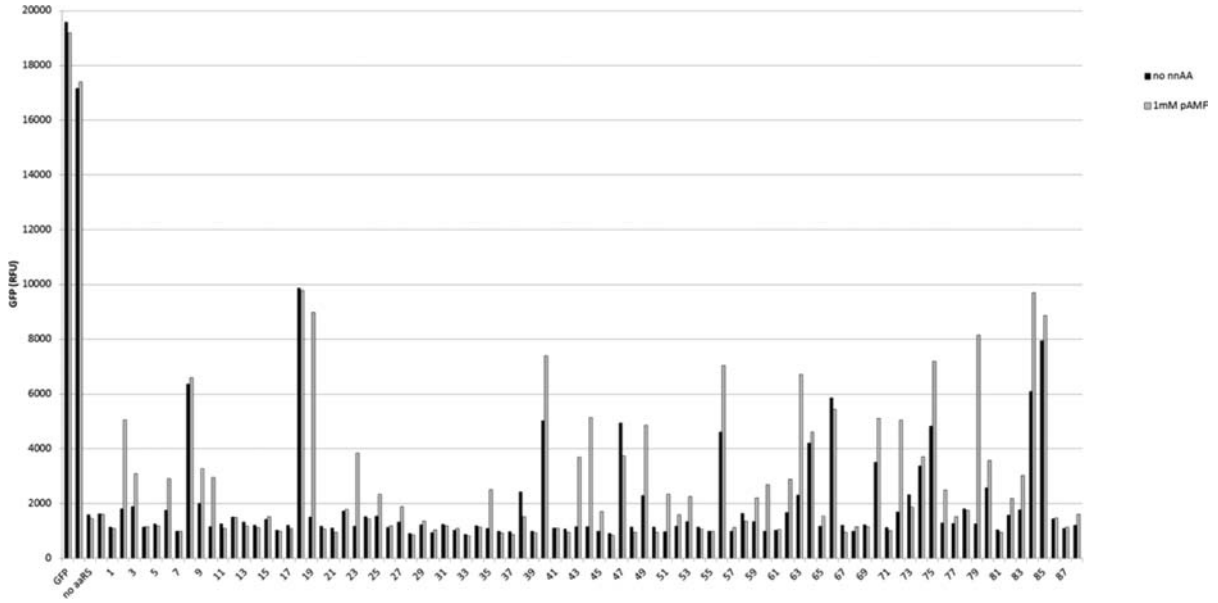

Figure 3. GFP TAG codon suppression-based screen for aaRS specificity toward pAMF. GFP suppression data from 1 screening plate. OCFS reactions expressing aaRS variants were added to a second set of reactions expressing GFP with a TAG codon at position 49 (GFP (K49TAG)). GFP TAG suppression reactions were performed in the absence (no nnAA) or presence of 1 mM pAMF. GFP fluorescence was measured after 12 h at 30 °C. Positive control reactions expressed GFP with no amber codon (GFP) and negative control reactions expressed GFP (K49TAG) with no synthetase expression reaction added.

A

pAMFRS variant	Residue # 32	65	108	109	158	159	$GFP^{1mM\ pAMF}$ / $GFP^{No\ pAMF}$	IgG HC 136-AB36267 DAR	EC50 (nM)
B03	A	V	W	Q	A	G	11.5	1.9	0.043
D08	T	V	W	Q	A	S	11.3	1.8	0.044
C10	V	V	Y	Q	A	V	8.9	1.6	0.048
A04	V	A	W	M	A	G	8.9	1.5	0.047
C02	V	V	W	I	A	S	7.7	1.5	0.044
A01	T	A	Y	L	A	S	4.7	1.2	0.071

B

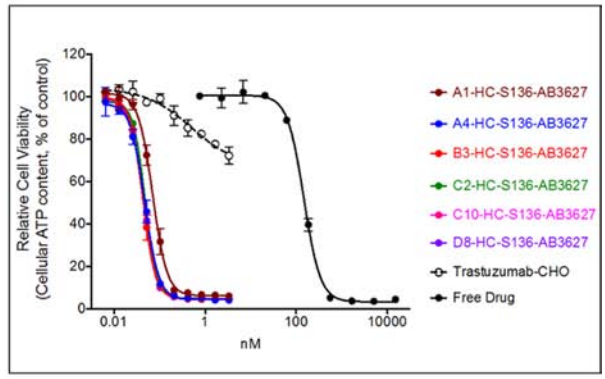

C

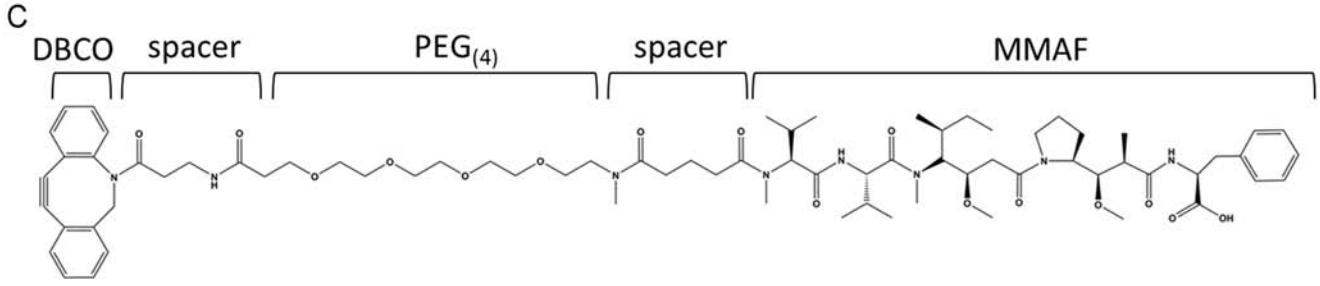

Figure 4. pAMF-specific TyrRS variants produce potent ADCs with high DAR values. (A) Top-ranking pAMFRS variants shown with the selected residues at library positions. $GFP^{1\ mM\ pAMF}$/$GFP^{No\ pAMF}$ ratios from secondary screen GFP (TAG) suppression reactions. DAR values, determined by mass spectrometry, of Trastuzumab HC 136-MMAF ADCs produced with top-ranking pAMFRS synthetases. EC_{50} values for ADCs produced with each pAMFRS were determined by titration on Her2-postive SKBR3 cells (B) followed by cell viability measurement using the Cell Titer-Glo assay (Promega). (C) Structure of DBCO-PEG-MMAF payload conjugated to pAMF at Trastuzumab heavy chain position 136.

In order to create a library of aaRS variants, purified plasmid DNA from 1760 individual colonies was used as a DNA template for T7 DNA polymerase driven aaRS expression, and arrayed as 100 μL OCFS reactions in 96-well microtiter plates. These protein synthesis reactions were used as a source of aaRS for the second set of OCFS reactions—to support nnAA incorporation into a GFP reporter though amber codon suppression. The amber suppression reporter reactions expressed GFP with an amber TAG codon at lysine 49 of Superfolder GFP.[42] Lysine 49 is in a solvent-exposed loop, and is a permissive site that allows for GFP fluorescence regardless of the amino acid present at this position. Comparison of GFP

dx.doi.org/10.1021/bc400490z | Bioconjugate Chem. 2014, 25, 351−361

fluorescence in the presence of pAMF versus the absence of pAMF would indicate specific aaRS activity toward the nnAA and the ability to discriminate against the 20 natural amino acids. We performed the amber suppression reporter reactions in a cell extract that contained an amber suppressor tRNA which is recognized by *M. jannaschii* TyrRS and has been optimized for high expression and low toxicity in our extract strain. Reactions were performed in the absence of pAMF or in the presence of 1 mM pAMF at 30 °C for 12 h in 384 well microtiter plates, followed by measurement of GFP fluorescence. In this primary screen, synthetase variants were identified with a large spectrum of activity and specificity. There were many nonfunctional clones that failed to support GFP amber suppression in either the presence or absence of pAMF (Figure 3A, clones 1, 4, 5, and 7). There were also several active but nonspecific clones that mediated efficient amber suppression in both the presence and absence of pAMF (Figure 3A, clones 8, 18, and 85). Importantly, this screen identified several unique clones that supported a high degree of GFP amber suppression only in the presence of pAMF (Figure 3A, clones 19, 44, and 79). These clones are predicted to have high selectivity for the nnAA pAMF while discriminating against the 20 natural amino acids. Roughly 7% of synthetase clones had the desired high activity and selectivity toward pAMF, exhibiting at least 3-fold higher suppression efficiency in the presence of pAMF than in the absence of pAMF (Figure S3).

The pAMF-specific aaRS (pAMFRS) clones were rank-ordered based on the ratio of the GFP signal in the presence of pAMF versus the absence of pAMF (Figure S3). Plasmid DNA from the top 192 clones was submitted for DNA sequencing. Several top-ranking sequences appeared several times, validating our screen and confirming our calculations that we had sampled the entire library diversity more than once. We selected 44 unique clones that exhibited the highest activity and specificity toward pAMF. Plasmid DNA for these clones was purified and rearrayed for secondary screening. OCFS reaction conditions for secondary screening were identical to those for the primary screen. Interestingly, 41 of 44 clones supported significantly more GFP amber suppression in the presence of 1 mM pAMF than in its absence (Figure S4). A majority of clones supported very high suppression efficiencies in the presence of pAMF and background levels of suppression or GFP fluorescence in reactions lacking pAMF. We transferred the top 6 clones from this screen into a final validation test using purified pAMFRS enzymes.

Production of Site-Specific pAMF-Containing ADCs. For a final characterization, we sought to confirm functional activity and fidelity of the top-ranking pAMFRS clones through nnAA incorporation into the Her2-specific monoclonal antibody Trastuzumab (Roche). We designed a DBCO-PEG-monomethyl auristatin (DBCO-PEG-MMAF) drug-linker compound that would enable conjugation of pAMF-incorporated antibody to the toxic payload. The features of the drug-linker compound are illustrated in Figure 4C and include a DBCO moiety to enable conjugation to pAMF, a noncleavable PEG linker, and the microtubule-disrupting antimitotic agent MMAF.[43] Since the linker we designed is noncleavable and serum stable (unpublished results), the most probable route for intracellular drug release is via lysosomal degradation. This degradative route would liberate the pAMF amino acid-conjugated DBCO-PEG-MMAF warhead, as has been demonstrated for other ADCs with noncleavable linkers.[44] It has previously been demonstrated that noncleavable MMAF drug-linker payloads can be used to produce highly potent ADCs.[45] The six top-ranked synthetases were expressed in OCFS at the 1 mL scale and directly purified using Ni-IMAC PhyTips on an Oasis liquid handling workstation. Purified protein was quantified using microfluidic gel electrophoresis on a Caliper LabChip GXII instrument (Perkin-Elmer). Purified synthetase protein was added to a nnAA-IgG expression reaction at a final concentration of 2 μM. Plasmid DNAs encoding the heavy chain (HC) with an amber codon at position 136 (HC-S136TAG) and untagged light chain of Trastuzumab IgG1 were added to the cell-free reaction at a ratio of 3:1, respectively. The S136 position was chosen based on examination of the suppression efficiency (Figure S5), conjugation efficiency, and potency of many possible conjugation sites throughout the solvent-exposed surface area of the Trastuzumab IgG scaffold (unpublished results). We also confirmed that pAMF conferred improved SPAAC conjugation kinetics, relative to the pAzF when the respective nnAA was incorporated at position 136 in the Trastuzumab heavy chain (Figure S6), consistent with our small molecule conjugation kinetic analysis. Cell-free expression reactions were performed in the presence of 1 mM pAMF, as in the primary and secondary screening reactions. Full-length heavy chain with a C-terminal hexahistidine tag, and thus fully assembled IgG, could be produced only by suppression of the TAG codon and at position 136 (Kabat numbering). Full-length assembled IgG protein was purified with Ni-IMAC PhyTips and the 150 kDa species was quantitated by Caliper. Expression titers were estimated at approximately 250 μg/mL. Since all of the selected pAMFRS variants exhibited high specific activity toward pAMF in primary and secondary screens, we reasoned that the IgGs produced in these reactions had a very high percentage of pAMF incorporated at HC position 136. The purified, nnAA-incorporated Trastuzumab antibodies were conjugated to a DBCO-PEG-monomethyl auristatin (DBCO-PEG-MMAF) compound (Figure 4C) in copper-free click conjugation reactions to produce complete antibody−drug conjugates. Drug conjugation did not cause any dissociation or aggregation of the intact IgG scaffold as determined by analytical size-exclusion chromatography (Figure S7). These antibody−drug conjugates were assayed for the extent of drug conjugation, or drug-to-antibody ratio (DAR) by mass spectrometry analysis of intact protein conjugates. DAR values were calculated as the weighted average of the deconvoluted mass spectrum peak intensities for each IgG drug−linker conjugate species (i.e., DAR 0, 1, and 2). In general, we observed very high degrees of conjugation with DAR values ranging from a low of 1.2 to a high of 1.9 that correlated well with the activity and specificity of the pAMFRS variant used to produce each respective ADC sample (Figure 4A).

In Vitro Cytotoxicity of ADCs. Since we used the Her2-specific Trastuzumab IgG scaffold to construct our ADCs, we performed cell killing analyses of our ADCs using the Her2-positive breast cancer cell line SKBR3, a model system used to validate other Trastuzumab-based ADCs. Auristatin-loaded ADCs as well as unconjugated Trastuzumab were incubated on SKBR3 cells at various concentrations for 5 days and specific cytotoxicity measured by a luminescence-based cell viability assay (Figure 4B). Compared to unconjugated Trastuzumab, which is ineffective at cell killing at the concentrations tested, and unconjugated free MMAF drug (EC_{50}−100nM) the Trastuzumab HC136-MMAF conjugates exhibited potent

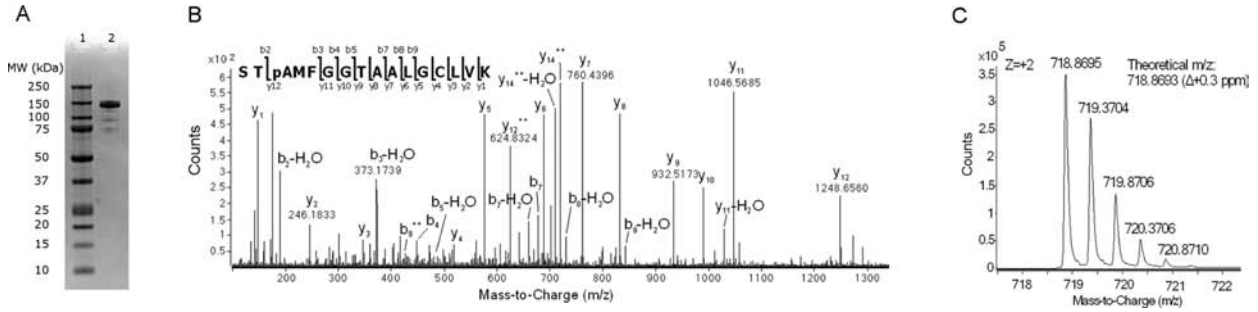

Figure 5. High fidelity pAMF incorporation at Trastuzumab HC position 136. (A) pAMFRS B03 was used to produce Trastuzumab HC-S136pAMF which was purified to >90% homogeneity for MS analysis. (B) Tandem MS spectrum of the Trastuzumab HC-S136pAMF tryptic peptide containing pAMF. The presence of pAMF is verified by its presence in multiple product ions. All indicated ions match their theoretical m/z values within $m/z \pm 0.02$. Parent ion: m/z 718.8715 m/z, $Z = 2$. (C) Zoomed mass spectrum of the Trastuzumab HC-S136pAMF tryptic peptide containing the non-native amino acid. The +1 and +3 charge states were also observed at m/z 1436.729 (−2.0 ppm) and m/z 479.5824 (+0.8 ppm), respectively.

cytotoxicity with EC_{50} values ranging from 0.043 nM to 0.071 nM (Figure 4A). These values are in good agreement with published EC_{50} values for Trastuzumab-DM1 ADCs generated by random conjugation methods.[46] The potency of these ADCs correlated well with the DAR value (Figure 4A). Importantly, these ADCs were not cytotoxic when tested on Her2-negative cell line MDA-MB-468 or MCF-7 (Figure S9). This indicates that excess drug-linker used during conjugation was effectively cleared post conjugation and that specific targeting and increased potency of the drug-linker were Her2 antigen-specific.

High Fidelity pAMF Incorporation. The high degree of amber codon suppression that was observed only in the presence of pAMF, the high ADC DAR value, and high drug potency mediated by pAMFRS variant B03 (Figure 4) all together indicated that this synthetase variant possessed a high degree of specificity for pAMF. The difference in DAR between the 6 Trastuzumab preps produced with the 6 different synthetases (Figure 4) is most likely attributable to differences in the efficiency and specificity of pAMF incorporation. This is for several reasons: (1) the site of pAMF incorporation was the same, so positional effects that can lead to variable conjugation efficiency are not a factor; (2) the conjugation reactions proceeded for 16 h, past the time point at which the ADC conjugation reaction has plateaued (Figure S6); and (3) the mass spectrometric method of DAR analysis offers very accurate and robust analysis, making inaccuracy of measurement highly unlikely, and (4) the observed DAR and EC_{50} values correlate very well with the activity/specificity ratio ($GFP^{1\ mM\ pAMF}/GFP^{No\ pAMF}$, Figure 4A) of the synthetase variant used to produce each ADC. It thus seems most likely that the lower DAR samples are the result of misincorporation events by lower fidelity synthetases, which lead to production of full-length HC species with natural amino acids at position 136 that cannot react with the DBCO drug linker. To follow up on pAMFRS incorporation fidelity, mass spectrometry analysis was used as a high resolution method to determine the precise fidelity of pAMFRS variant B03. Aminoacyl tRNA synthetase fidelity percentage can be defined as the frequency with which the enzyme charges its cognate tRNA with its cognate amino acid versus any other amino acid. To derive this number, we measured the frequency of pAMF incorporation versus any other amino acids at the position 136 TAG codon in the Trastuzumab heavy chain. Trastuzumab HC S136-TAG was coexpressed with Trastuzumab LC in the presence of pAMFRS variant B03, amber suppressor tRNA, and 1 mM pAMF in a 30 mL OCFS reaction. The full-length, assembled IgG was purified to >90% purity (Figure 5A and Figure S7) prior to tryptic digestion and mass spectrometry (MS) analysis of the pAMF-incorporated HC peptide. MS data were acquired first with an MS-only method, followed by a data-dependent MS/MS method with preferential selection for the target tryptic peptides containing pAMF, Phe, Tyr, or Gln at position 136. We have previously observed Phe, Tyr, and Gln misincorporation when using other amber suppression systems and as endogenous amber suppression events involving mismatch decoding of TAG codons by endogenous tRNAs. The tandem MS of the Trastuzumab HC-S136pAMF tryptic peptide positively identified the presence of pAMF at position 136 (Figure 5B and C). In addition, tryptic peptides containing Phe, Tyr, or Gln at HC position 136 and all other Phe positions in the protein could not be detected above the spectral noise level. Furthermore, we observed no measurable nonsuppressed S136TAG truncation product in a parallel OCFS reaction containing ^{14C}Leu, which indicates a high degree of pAMF incorporation (Figure S5). Since no misincorporated peptides were observed, the maximum rate of misincorporation would be the noise level, or limit of detection of our MS method. Fidelity percentage was calculated as the ratio of the signal intensity for the pAMF-incorporated target peptide to the spectral noise intensity at the expected position of a Phe, Tyr, or Gln-containing target peptide to yield a fidelity percentage of at least 99.8% for pAMFRS variant B03 (Table S1). We do observe a small amount of full-length Trastuzumab synthesized in the absence of pAMFRS (Figure S5), presumably due to amber suppression events attributable to mismatch decoding of the TAG codon by endogenous tyrosine and glutamine-charged tRNAs (TAT/TAC, and CAG-decoding tRNAs, respectively). However, these misincorporation events were not observed on our LC-MS/MS-based peptide analysis. This suggests that such endogenous amber suppression events occur very rarely, if at all, in the presence of the highly efficient pAMF-based amber suppression system described herein.

DISCUSSION

We have discovered several aminoacyl tRNA synthetases, derived from the *M. jannaschii* TyrRS, that mediate efficient and faithful cotranslational incorporation of the optimized non-native amino acid para-azidomethyl-L-phenylalanine into proteins expressed in our OCFS system. These novel pAMFRS enzymes were discovered through a direct library screening approach that leveraged the high-throughput and scalable nature of our in vitro protein expression platform. This direct

dx.doi.org/10.1021/bc400490z | Bioconjugate Chem. 2014, 25, 351−361

screening approach can be applied to other nnAA-aaRS systems and presumably other protein engineering challenges. We can now expand the repertoire of nnAAs available for incorporation and conjugation by redirecting tRNA synthetase activity toward the nnAA of our design. These may include amino acids with optimized solubility, which could limit potential detrimental effects of nnAA incorporation on protein folding or solubility. We will also explore nnAAs that could offer access to additional bio-orthogonal conjugation chemistries. Such capabilities could pave the way for ADCs with multiple different warheads with distinct cytotoxic modes of action, a true targeted combination chemotherapeutic.

This open nature of this coupled *in vitro* transcription/translation system allows exquisite control over the relative ratio of natural to non-natural amino acids, unlike traditional *in vivo* approaches. Because of this, we may be able to drive enzymes with less inherent specificity for the nnAA toward higher fidelity incorporation, simply by providing excess nnAA. Another advantage of our screening approach is that no intact living cells are used. As a result, future synthetase screens could be directed toward nnAAs that exhibit toxicity or membrane permeability challenges that preclude their use in traditional in vivo-based synthetase selection systems.

Another important consideration is that, unlike protein therapeutics produced in eukaryotic expression systems, proteins synthesized in our system are aglycosylated, it will be imperative to compare the stability, efficacy, and pharmacokinetic properties of proteins produced in this prokaryotic-based cell-free system to glycosylated benchmark molecules. If these properties are maintained, the lack of heterogeneous glycan linkages may streamline characterization and purification of molecules expressed using OCFS.

In comparison to the previously utilized para-azido-L-phenylalanine, pAMF has an enhanced rate of conjugation in copper-free click reactions, and is less prone to reduction.[41] With this optimized aaRS-tRNA-nnAA system, we can produce pAMF-containing proteins that will have more robust post-translational conjugation profiles, a key consideration for both research and manufacturing settings. This enhanced nnAA incorporation and conjugation system will enable exhaustive studies of nnAA-mediated protein conjugates. Because our in vitro expression system can produce high yields of high quality site-specifically nnAA incorporated material, we can rapidly perform comprehensive analyses of the relationships between the site of nnAA incorporation/conjugation and protein attributes such as aggregation state, stability, target binding, and cell killing studies. Such studies, enabled by our ADC production and screening platform, have the potential to yield a second generation of best-in-class, site-specific ADCs with superior therapeutic properties and product homogeneity could conceivably be ushered more rapidly from proof-of-concept through clinical trials, to an FDA-approved, bona fide oncology therapeutic.

■ ASSOCIATED CONTENT

Supporting Information

Supplemental Experimental Procedures. Chemical synthesis schemes for pAMF and DBCO-PEG-MMAF. Rank-ordered overview of pAMFRS screen output. GFP (K49TAG) suppression analysis of 44 clones selected for secondary screening. SDS-PAGE autoradiography analysis of nnAA-containing IgG expression in OCFS. Conjugation kinetics of drug-linker on nnAA-containing Trastuzumab. Analytical size-exclusion chromatography analysis of ADCs before and after drug linker conjugation. Deconvoluted mass spectrum of a site-specific, pAMF-mediated ADC. ADC cytotoxicity analysis on Her2 positive and Her2-negative cell lines. This material is available free of charge via the Internet at http://pubs.acs.org.

■ AUTHOR INFORMATION

Corresponding Author

*E-mail: asato@sutrobio.com. Phone: 650-392-8412. Fax: 650-872-8924.

Notes

The authors declare no competing financial interest.

■ REFERENCES

(1) Younes, A., Bartlett, N. L., Leonard, J. P., Kennedy, D. A., Lynch, C. M., Sievers, E. L., and Forero-Torres, A. (2010) Brentuximab vedotin (SGN-35) for relapsed CD30-positive lymphomas. *N. Engl. J. Med. 363*, 1812−1821.

(2) Verma, S., Miles, D., Gianni, L., Krop, I. E., Welslau, M., Baselga, J., Pegram, M., Oh, D.-Y., Diéras, V., Guardino, E., Fang, L., Lu, M. W., Olsen, S., Blackwell, K., et al. (2012) Trastuzumab emtansine for HER2-positive advanced breast cancer. *N. Engl. J. Med. 367*, 1783−1791.

(3) Shen, B.-Q., Xu, K., Liu, L., Raab, H., Bhakta, S., Kenrick, M., Parsons-Reponte, K. L., Tien, J., Yu, S.-F., Mai, E., Li, D., Tibbitts, J., Baudys, J., Saad, O. M., Scales, S. J., McDonald, P. J., Hass, P. E., Eigenbrot, C., Nguyen, T., Solis, W. A., Fuji, R. N., Flagella, K. M., Patel, D., Spencer, S. D., Khawli, L. A., Ebens, A., Wong, W. L., Vandlen, R., Kaur, S., Sliwkowski, M. X., Scheller, R. H., Polakis, P., and Junutula, J. R. (2012) Conjugation site modulates the in vivo stability and therapeutic activity of antibody-drug conjugates. *Nat. Biotechnol. 30*, 184−189.

(4) Junutula, J. R., Raab, H., Clark, S., Bhakta, S., Leipold, D. D., Weir, S., Chen, Y., Simpson, M., Tsai, S. P., Dennis, M. S., Lu, Y., Meng, Y. G., Ng, C., Yang, J., Lee, C. C., Duenas, E., Gorrell, J., Katta, V., Kim, A., McDorman, K., Flagella, K., Venook, R., Ross, S., Spencer, S. D., Lee Wong, W., Lowman, H. B., Vandlen, R., Sliwkowski, M. X., Scheller, R. H., Polakis, P., and Mallet, W. (2008) Site-specific conjugation of a cytotoxic drug to an antibody improves the therapeutic index. *Nat. Biotechnol. 26*, 925−932.

(5) Jeffrey, S. C., Burke, P. J., Lyon, R. P., Meyer, D. W., Sussman, D., Anderson, M., Hunter, J. H., Leiske, C. I., Miyamoto, J. B., Nicholas, N. D., Okeley, N. M., Sanderson, R. J., Stone, I. J., Zeng, W., Gregson, S. J., Masterson, L., Tiberghien, A. C., Howard, P. W., Thurston, D. E., Law, C.-L., and Senter, P. D. (2013) A potent anti-CD70 antibody−drug conjugate combining a dimeric pyrrolobenzodiazepine drug with site-specific conjugation technology. *Bioconjugate Chem. 24*, 1256−1263.

(6) Agarwal, P., van der Weijden, J., Sletten, E. M., Rabuka, D., and Bertozzi, C. R. (2013) A Pictet-Spengler ligation for protein chemical modification. *Proc. Natl. Acad. Sci. U. S. A. 110*, 46−51.

(7) Strop, P., Liu, S.-H., Dorywalska, M., Delaria, K., Dushin, R. G., Tran, T.-T., Ho, W.-H., Farias, S., Casas, M. G., Abdiche, Y., Zhou, D., Chandrasekaran, R., Samain, C., Loo, C., Rossi, A., Rickert, M., Krimm, S., Wong, T., Chin, S. M., Yu, J., Dilley, J., Chaparro-Riggers, J., Filzen, G. F., O'Donnell, C. J., Wang, F., Myers, J. S., Pons, J., Shelton, D. L., and Rajpal, A. (2013) Location matters: site of conjugation modulates stability and pharmacokinetics of antibody drug conjugates. *Chem. Biol. 20*, 161−167.

(8) Axup, J. Y., Bajjuri, K. M., Ritland, M., Hutchins, B. M., Kim, C. H., Kazane, S. A., Halder, R., Forsyth, J. S., Santidrian, A. F., Stafin, K., Lu, Y., Tran, H., Seller, A. J., Biroc, S. L., Szydlik, A., Pinkstaff, J. K., Tian, F., Sinha, S. C., Felding-Habermann, B., Smider, V. V., and Schultz, P. G. (2012) Synthesis of site-specific antibody-drug conjugates using unnatural amino acids. *Proc. Natl. Acad. Sci. U. S. A. 109*, 16101−16106.

(9) Wang, L., Brock, A., Herberich, B., and Schultz, P. G. (2001) Expanding the genetic code of Escherichia coli. *Science 292*, 498−500.
(10) Wang, L., Xie, J., and Schultz, P. G. (2006) Expanding the genetic code. *Annu. Rev. Biophys. Biomol. Struct. 35*, 225−249.
(11) Young, T. S., and Schultz, P. G. (2010) Beyond the canonical 20 amino acids: expanding the genetic lexicon. *J. Biol. Chem. 285*, 11039−11044.
(12) Chin, J. W., Cropp, T. A., Anderson, J. C., Mukherji, M., Zhang, Z., and Schultz, P. G. (2003) An expanded eukaryotic genetic code. *Science 301*, 964−967.
(13) Anderson, J. C., and Schultz, P. G. (2003) Adaptation of an orthogonal archaeal leucyl-tRNA and synthetase pair for four-base, amber, and opal suppression. *Biochemistry (Mosc.) 42*, 9598−9608.
(14) Santoro, S. W., Anderson, J. C., Lakshman, V., and Schultz, P. G. (2003) An archaebacteria-derived glutamyl-tRNA synthetase and tRNA pair for unnatural amino acid mutagenesis of proteins in Escherichia coli. *Nucleic Acids Res. 31*, 6700−6709.
(15) Nguyen, D. P., Lusic, H., Neumann, H., Kapadnis, P. B., Deiters, A., and Chin, J. W. (2009) Genetic encoding and labeling of aliphatic azides and alkynes in recombinant proteins via a pyrrolysyl-tRNA Synthetase/tRNA(CUA) pair and click chemistry. *J. Am. Chem. Soc. 131*, 8720−8721.
(16) Yanagisawa, T., Ishii, R., Fukunaga, R., Kobayashi, T., Sakamoto, K., and Yokoyama, S. (2008) Multistep engineering of pyrrolysyl-tRNA synthetase to genetically encode N(epsilon)-(o-azidobenzyloxycarbonyl) lysine for site-specific protein modification. *Chem. Biol. 15*, 1187−1197.
(17) Santoro, S. W., Wang, L., Herberich, B., King, D. S., and Schultz, P. G. (2002) An efficient system for the evolution of aminoacyl-tRNA synthetase specificity. *Nat. Biotechnol. 20*, 1044−1048.
(18) Young, T. S., Ahmad, I., Yin, J. A., and Schultz, P. G. (2010) An enhanced system for unnatural amino acid mutagenesis in E. coli. *J. Mol. Biol. 395*, 361−374.
(19) Melançon, C. E., 3rd, and Schultz, P. G. (2009) One plasmid selection system for the rapid evolution of aminoacyl-tRNA synthetases. *Bioorg. Med. Chem. Lett. 19*, 3845−3847.
(20) Liu, W., Brock, A., Chen, S., Chen, S., and Schultz, P. G. (2007) Genetic incorporation of unnatural amino acids into proteins in mammalian cells. *Nat. Methods 4*, 239−244.
(21) Cho, H., Daniel, T., Buechler, Y. J., Litzinger, D. C., Maio, Z., Putnam, A.-M. H., Kraynov, V. S., Sim, B.-C., Bussell, S., Javahishvili, T., Kaphle, S., Viramontes, G., Ong, M., Chu, S., Becky, G. C., Lieu, R., Knudsen, N., Castiglioni, P., Norman, T. C., Axelrod, D. W., Hoffman, A. R., Schultz, P. G., DiMarchi, R. D., and Kimmel, B. E. (2011) Optimized clinical performance of growth hormone with an expanded genetic code. *Proc. Natl. Acad. Sci. U. S. A. 108*, 9060−9065.
(22) Lee, H. S., Spraggon, G., Schultz, P. G., and Wang, F. (2009) Genetic incorporation of a metal-ion chelating amino acid into proteins as a biophysical probe. *J. Am. Chem. Soc. 131*, 2481−2483.
(23) Chin, J. W., Santoro, S. W., Martin, A. B., King, D. S., Wang, L., and Schultz, P. G. (2002) Addition of p-azido-L-phenylalanine to the genetic code of Escherichia coli. *J. Am. Chem. Soc. 124*, 9026−9027.
(24) Wang, L., Brock, A., and Schultz, P. G. (2002) Adding L-3-(2-Naphthyl)alanine to the genetic code of E. coli. *J. Am. Chem. Soc. 124*, 1836−1837.
(25) Wang, L., Zhang, Z., Brock, A., and Schultz, P. G. (2003) Addition of the keto functional group to the genetic code of Escherichia coli. *Proc. Natl. Acad. Sci. U. S. A. 100*, 56−61.
(26) Wu, N., Deiters, A., Cropp, T. A., King, D., and Schultz, P. G. (2004) A genetically encoded photocaged amino acid. *J. Am. Chem. Soc. 126*, 14306−14307.
(27) Bose, M., Groff, D., Xie, J., Brustad, E., and Schultz, P. G. (2006) The incorporation of a photoisomerizable amino acid into proteins in E. coli. *J. Am. Chem. Soc. 128*, 388−389.
(28) Jones, D. H., Cellitti, S. E., Hao, X., Zhang, Q., Jahnz, M., Summerer, D., Schultz, P. G., Uno, T., and Geierstanger, B. H. (2010) Site-specific labeling of proteins with NMR-active unnatural amino acids. *J. Biomol. NMR 46*, 89−100.
(29) Schultz, K. C., Supekova, L., Ryu, Y., Xie, J., Perera, R., and Schultz, P. G. (2006) A genetically encoded infrared probe. *J. Am. Chem. Soc. 128*, 13984−13985.
(30) Tsao, M.-L., Summerer, D., Ryu, Y., and Schultz, P. G. (2006) The genetic incorporation of a distance probe into proteins in Escherichia coli. *J. Am. Chem. Soc. 128*, 4572−4573.
(31) Nairn, N. W., Shanebeck, K. D., Wang, A., Graddis, T. J., VanBrunt, M. P., Thornton, K. C., and Grabstein, K. (2012) Development of copper-catalyzed azide-alkyne cycloaddition for increased in vivo efficacy of interferon β-1b by site-specific PEGylation. *Bioconjugate Chem. 23*, 2087−2097.
(32) Zawada, J. F., Yin, G., Steiner, A. R., Yang, J., Naresh, A., Roy, S. M., Gold, D. S., Heinsohn, H. G., and Murray, C. J. (2011) Microscale to manufacturing scale-up of cell-free cytokine production–a new approach for shortening protein production development timelines. *Biotechnol. Bioeng. 108*, 1570−1578.
(33) Yin, G., Garces, E. D., Yang, J., Zhang, J., Tran, C., Steiner, A. R., Roos, C., Bajad, S., Hudak, S., Penta, K., Zawada, J., Pollitt, S., and Murray, C. J. (2012) Aglycosylated antibodies and antibody fragments produced in a scalable in vitro transcription-translation system. *mAbs 4*, 217−225.
(34) Goerke, A. R., and Swartz, J. R. (2009) High-level cell-free synthesis yields of proteins containing site-specific non-natural amino acids. *Biotechnol. Bioeng. 102*, 400−416.
(35) Ozawa, K., Loscha, K. V., Kuppan, K. V., Loh, C. T., Dixon, N. E., and Otting, G. (2012) High-yield cell-free protein synthesis for site-specific incorporation of unnatural amino acids at two sites. *Biochem. Biophys. Res. Commun. 418*, 652−656.
(36) Loscha, K. V., Herlt, A. J., Qi, R., Huber, T., Ozawa, K., and Otting, G. (2012) Multiple-site labeling of proteins with unnatural amino acids. *Angew. Chem., Int. Ed. Engl. 51*, 2243−2246.
(37) Baskin, J. M., Prescher, J. A., Laughlin, S. T., Agard, N. J., Chang, P. V., Miller, I. A., Lo, A., Codelli, J. A., and Bertozzi, C. R. (2007) Copper-free click chemistry for dynamic in vivo imaging. *Proc. Natl. Acad. Sci. U. S. A. 104*, 16793−16797.
(38) Zawada, J. F. (2012) Preparation and testing of E. coli S30 in vitro transcription translation extracts. *Methods Mol. Biol. (Totowa, NJ, U. S.) 805*, 31−41.
(39) Jewett, J. C., and Bertozzi, C. R. (2010) Cu-free click cycloaddition reactions in chemical biology. *Chem. Soc. Rev. 39*, 1272−1279.
(40) Ning, X., Guo, J., Wolfert, M. A., and Boons, G.-J. (2008) Visualizing metabolically-labeled glycoconjugates of living cells by copper-free and fast Huisgen cycloadditions. *Angew. Chem., Int. Ed. Engl. 47*, 2253−2255.
(41) Bazewicz, C. G., Liskov, M. T., Hines, K. J., and Brewer, S. H. (2013) Sensitive, site-specific, and stable vibrational probe of local protein environments: 4-azidomethyl-l-phenylalanine. *J. Phys. Chem. B 117*, 8987−8993.
(42) Fisher, A. C., and DeLisa, M. P. (2008) Laboratory evolution of fast-folding green fluorescent protein using secretory pathway quality control. *PloS One 3*, e2351.
(43) Doronina, S. O., Mendelsohn, B. A., Bovee, T. D., Cerveny, C. G., Alley, S. C., Meyer, D. L., Oflazoglu, E., Toki, B. E., Sanderson, R. J., Zabinski, R. F., Wahl, A. F., and Senter, P. D. (2006) Enhanced activity of monomethylauristatin F through monoclonal antibody delivery: effects of linker technology on efficacy and toxicity. *Bioconjugate Chem. 17*, 114−124.
(44) Erickson, H. K., Park, P. U., Widdison, W. C., Kovtun, Y. V., Garrett, L. M., Hoffman, K., Lutz, R. J., Goldmacher, V. S., and Blättler, W. A. (2006) Antibody-maytansinoid conjugates are activated in targeted cancer cells by lysosomal degradation and linker-dependent intracellular processing. *Cancer Res. 66*, 4426−4433.
(45) Oflazoglu, E., Stone, I. J., Gordon, K., Wood, C. G., Repasky, E. A., Grewal, I. S., Law, C.-L., and Gerber, H.-P. (2008) Potent anticarcinoma activity of the humanized anti-CD70 antibody h1F6 conjugated to the tubulin inhibitor auristatin via an uncleavable linker. *Clin. Cancer Res. Off. J. Am. Assoc. Cancer Res. 14*, 6171−6180.

(46) Lewis Phillips, G. D., Li, G., Dugger, D. L., Crocker, L. M., Parsons, K. L., Mai, E., Blättler, W. A., Lambert, J. M., Chari, R. V. J., Lutz, R. J., Wong, W. L. T., Jacobson, F. S., Koeppen, H., Schwall, R. H., Kenkare-Mitra, S. R., Spencer, S. D., and Sliwkowski, M. X. (2008) Targeting HER2-positive breast cancer with trastuzumab-DM1, an antibody-cytotoxic drug conjugate. *Cancer Res. 68*, 9280−9290.